Proceedings of IMECE2003
2003 ASME International Mechanical Engineering Congress and Exposition
November 16-21, 2003, Washington, DC

IMECE2003-41386

SLIDING MODE CONTROL OF A NON-COLLOCATED FLEXIBLE SYSTEM

Aimee M. Frame
Intelligent Machine Dynamics Laboratory
Department of Mechanical Engineering
The Georgia Institute of Technology
Atlanta, GA 30332
Email: gtg414d@prism.gatech.edu

Wayne J. Book
Intelligent Machine Dynamics Laboratory
Department of Mechanical Engineering
The Georgia Institute of Technology
Atlanta, GA 30332
Email: wayne.book@me.gatech.edu

ABSTRACT

A new control method is developed for position tracking control of a flexible, non-collocated system. The desired trajectory is specified for the free end of a flexible beam that moves along a horizontal track actuated by a linear motor. First, a system model is reformulated based on a pendulum with stiffness and dampening. Small angle approximations are used so that a linear model can be obtained. Next, variable structure control is chosen as the control method due to its seemingly robust nature. The sliding surface and feedback gains are designed using the developed model based on literature describing various variable structure control techniques. Simulations are then conducted to verify the control method and examine its robustness. Finally, the method is implemented on an actual system using a Kalman filter to estimate the states.

Introduction

A major goal for industrial machinery has been to increase motion speed without sacrificing precision, leading to increased interest in control schemes that are aimed at improving the performance of lightweight, flexible machinery. There have been some recently developed algorithms, such as command shaping and adaptive learning control, that attempt to improve the motion control of flexible systems. These algorithms generally address collocated systems in which the sensors and actuators are at the same place. However, to address the exact placement of the mechanism's end-of-arm, a non-collocated system usually arises.

CAMotion Inc. has been investigating this problem for a lightweight, flexible manipulator that is prismatically actuated by a linear motor. The main objective of the work has been to move the end-of-arm through a desired periodic reference trajectory while minimizing error and vibration. Up to this point, this has been achieved through the use of command shaping and learning control in conjunction with a PID controller that uses encoder data from the motor.

In the recent past, CAMotion examined the use of a Kalman filter to estimate the end-of-arm position based on accelerometer feedback at the tip. During the investigation, a machine vision system was used for verification. Since machine vision systems are more readily available in industry, CAMotion would like to incorporate them into a state-feedback control strategy. An accelerometer is still used so that the control algorithm can utilize the best aspects of each sensor.

The application of variable structure control (VSC) to flexible systems has become of growing interest in the past decade due to the increased interest in the advantages of flexible robots over their rigid counterparts. Most of the work uses a flexible beam that rotates in a horizontal plane [1–4]. VSC has also been compared to other control methods, such as pole placement [5] and singular perturbation [6]. In addition to performance, robustness comparisons have also been made [7]. These comparisons have led to the conclusions that VSC is more robust and performs better than other control methods. Since robustness is an important issue to this research, VSC became the control strategy of interest.

The rest of this paper details the application of VSC to the flexible link problem posed by CAMotion. First, the modeling

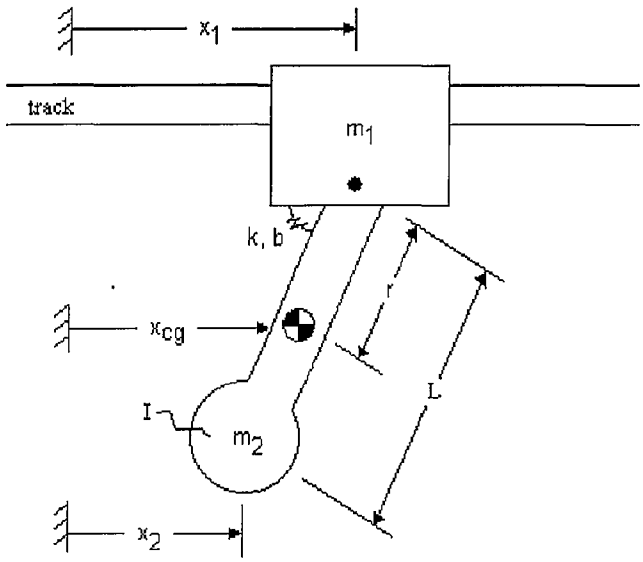

Figure 1. Model Schematic

of the system is described. Next is a brief discussion of the VSC techniques used in this research. The simulation and experimental methods and results are then discussed. Finally, conclusions based on the results shown are discussed.

System Model

Though mode shape analysis is widely used in flexible link problems, a different modeling approach was used for this problem. The previous work done by CAMotion used a lumped mass-spring-damper approach [8]. However, concern that the configuration used in the previous research may not represent possible non-minimum phase behavior of a robotic manipulator led to the development of a pendulum-type configuration. The resulting model can then be used in conjunction with the control formulation described in the next section to determine the necessary control gains.

The new model configuration, as shown in Figure 1, includes a base mass, m_1, that is constrained to move in the horizontal direction with the control force, F, acting on it. A tip mass is connected to m_1 by a long flexible beam. The mass of the beam and tip are considered to be a single inertial mass, m_2. Finally, torsional stiffness and damping are chosen to act at the connection point.

In order to derive the state-space representation of this new model the following set of differential equations is developed. Since the reaction force at the joint will not create a moment, only the horizontal reaction force, f, is needed.

$$m_1\ddot{x}_1 = F - f \tag{1}$$

$$m_2\ddot{x}_{cg} = f \tag{2}$$

$$I\ddot{\theta} = fr - k\theta - b\dot{\theta} \tag{3}$$

It is assumed that the motion of the second mass relative to the first is small so that small angle approximations for θ can be used. Choosing the states to be the mass positions and velocities, the following state space representation can be used.

$$\dot{X} = \begin{bmatrix} 0 & 0 & 1 & 0 \\ 0 & 0 & 0 & 1 \\ ak & -ak & ab & -ab \\ -ck & ck & -cb & cb \end{bmatrix} X + \begin{bmatrix} 0 \\ 0 \\ d \\ e \end{bmatrix} F \tag{4}$$

$$y = \begin{bmatrix} 1 & 0 & 0 & 0 \\ -ck & ck & -cb & cb \\ 0 & 0 \; or \; 1 & 0 & 0 \end{bmatrix} X + \begin{bmatrix} 0 \\ e \\ 0 \end{bmatrix} F \tag{5}$$

Where $X = [x_1 \quad x_2 \quad \dot{x}_1 \quad \dot{x}_2]^T$, $a = \frac{m_2 r}{\delta}$, $c = \frac{m_1 L + m_2 (L-r)}{\delta}$, $d = \frac{-L(I+m_2 r^2)}{\delta}$, $e = \frac{L[m_2 r(L-r)-I]}{\delta}$, and $\delta = -m_1 L(I + m_2 r^2) - m_2 I L$.

The term δ arises when the M matrix is inverted while solving for $\ddot{x}_1$ and $\ddot{x}_2$. Also, since a vision measurement is not available at all times, the last row of (5) will be zero except when there is a vision measurement.

Once the state-space representation is developed, it is desirable to have actual values for each of the system parameters. Table 1 lists the values, which were found experimentally. Also, the natural frequency of the beam when it is clamped at the joint was found to be 23 Hz. The transfer function between the tip position and the input was then calculated using these values so that the properties of the system could be examined. The poles are stable as expected from physical arguments. The zeros of the transfer function are also examined and are found to be in the left half plane. Therefore, the system is minimum phase which does not add complexity to the control design. However, since many of the parameters are not found by direct measurement, there is a great amount of uncertainty in the values obtained. Therefore, the controller design must be robust enough to handle these uncertainties as well as any other variations due to outside influences.

Parameters	Value
Base mass, m_1	8 kg
Tip mass, m_2	2.55 kg
Beam length, L	0.526 m
Distance to center of mass, r	0.377 m
Mass moment of inertia, I	0.4367 kgm^2
Spring constant, k	32,199 Nm
Damping coefficient, b	9.8863 Nms

Table 1. Pendulum Model Parameters

Variable Structure Control

Variable Structure Control (VSC) can be described as a switched feedback control method that drives a system trajectory to a specified surface in the state space. This surface, $\sigma = 0$, is called a *sliding surface* because ideally the plant's trajectory slides along it for all time once the surface is reached, which is referred to as a *sliding mode*. To reach the surface, the control gains are switched based on whether the states are "above" or "below" the sliding surface. Thus, the VSC design is a two-part process: the switching surface is designed first and then the switched feedback law [9].

Sliding Surface Design

Since the sliding surface design determines the behavior of the plant while in sliding mode, the design is based on the plant dynamics of the state space representation. For linear systems, a linear transformation, $z = TX$, into *regular form* is made. Regular form consists of partitioned matrices, as shown in (6) and (7), where B_2 and S_2 are square matrices of order equal to the number of inputs.

$$\begin{bmatrix} \dot{X}_1 \\ \dot{X}_2 \end{bmatrix} = \begin{bmatrix} A_{11} & A_{12} \\ A_{21} & A_{22} \end{bmatrix} \begin{bmatrix} X_1 \\ X_2 \end{bmatrix} + \begin{bmatrix} 0 \\ B_2 \end{bmatrix} u \tag{6}$$

$$\sigma = \begin{bmatrix} S_1 & S_2 \end{bmatrix} \begin{bmatrix} X_1 \\ X_2 \end{bmatrix} \tag{7}$$

Using the fact that it is desired that $\sigma = 0$, the sliding surface design problem now becomes that of a state feedback problem, $\dot{X}_1 = (A_{11} - A_{12}S_2^{-1}S_1)X_1$, where the state matrix is A_{11}, the input matrix is A_{12} and feedback gain is $-S_2^{-1}S_1$ [9]. This allows the use of conventional feedback methods, such as LQG, in the sliding surface design. For convenience, S_2 is usually set equal to the identity matrix so that S_1 is equal to the gain obtained from the feedback method used. Once the surface is found using regular form, it must be transformed so that it can be used with the original state space representation. Therefore, $\sigma = \hat{S}z = \hat{S}TX = SX$.

A linear-quadratic approach with a cost function of $J = \frac{1}{2}\int_{t_o}^{t_f}[X^T(t)QX(t) + u^T(t)ru(t)]dt$ was used to determine the sliding surface for this research. Since the control objective is to minimize position error of x_2, Q was chosen to be a $(n-1)^{th}$ order square matrix whose only non-zero term is the diagonal term associated with x_2, which is chosen to be a value greater than one. To further reduce the input cost, r is chosen to be a value less than one. If the system dynamics along the sliding surface are unsatisfactory, the surface can be redesigned using different Q and r values. For example, by increasing the non-zero value of Q, better position tracking control may be achieved.

Switched State Feedback Control Design

Once the sliding surface is determined, the next step is to design the switched feedback law that will drive the state trajectories to that surface. Since switching causes the problem to be non-linear, Lyapunov stability theory is used in the design process. This theory states that given a positive definite function, $V(x)$, the surface can be reached in a finite number of steps if $\dot{V}(x) < -\eta|s|$, where η is a strictly positive number [10]. However, for most practical applications, negative definiteness, $\dot{V}(x) < 0$, is a sufficiently convergent condition. The typical positive definite function used for single input systems is $V(x) = \frac{1}{2}\sigma^2(x)$, which leads to an inequality, (8), that needs to be satisfied to ensure stability.

$$\dot{V}(x) = \sigma S[AX + Bu] < 0 \tag{8}$$

The control gains are obtained by choosing a particular control structure and substituting it directly into (8). The general structure for a feedback controller with switched gains, (9), was chosen for this research, resulting in (10).

$$\begin{aligned} u &= g_1x_1 + g_2x_2 + \cdots + g_nx_n \\ &= KX \\ g_i &= \begin{cases} \alpha_i & \sigma x_i > 0 \\ \beta_i & \sigma x_i < 0 \end{cases} \end{aligned} \tag{9}$$

$$\dot{V}(x) = S[A + BK]\sigma X \tag{10}$$

Since it is desired to have a generic algorithm that can be used for any given set of state matrices with a single input, a process for calculating the controller gains based only on the state

matrices and sliding surface was developed. First, the right-hand side of (10) is said to be less than zero since it is a scalar. Noting that SB is also a scalar quantity for a single input, the equation can now be rewritten as follows.

$$SB\left[\frac{SA}{SB}+K\right]\begin{bmatrix}\sigma x_1\\ \sigma x_2\\ \vdots\\ \sigma x_n\end{bmatrix}<0 \tag{11}$$

A new variable, γ, is chosen such that $\gamma=\frac{-SA}{SB}$, which is a vector with the same dimensions as K. Thus, the coefficient of σx_i is $SB(-\gamma_i+K_i)$ which then leads to the following statements.

$$\begin{aligned}&\text{if } SB>0 \quad \alpha_i<\gamma_i \\ &\qquad\qquad\ \beta_i>\gamma_i \\ &\text{if } SB<0 \quad \alpha_i>\gamma_i \\ &\qquad\qquad\ \beta_i<\gamma_i\end{aligned} \tag{12}$$

This simplification only deals with single input systems, but the method can be extended to multi-input systems. First, a sliding surface is defined for each input, creating an S matrix with multiple rows. The gains for each input can then be determined using (12) where S is the row and B is the column corresponding to the input of interest. Thus, a general method to calculate the control gains has been derived for the control structure described by (9) for any given A, B, and S matrices. For further details on variable structure control, refer to [9, 11, 12].

Simulation

The electronic portion of the test system consists of a computer, Remote Axis Serial Interface Device (RASID), and amplifier. The RASID is a compact unit located close to the motor that contains a digital signal processor to control the motor's position. In this work, the computer is used as an operator interface

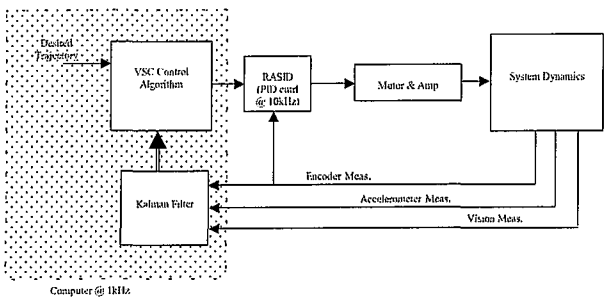

Figure 2. Control System Schematic

to the RASID and to do trajectory planning. The desired motor positions are sent to the RASID at a rate of 1 kHz. An internal PID routine in the RASID is used to calculate the control signal necessary to drive the error to zero using encoder measurements at 10 kHz. To implement state-feedback control, a Kalman filter and additional output measurements are added to create the overall schematic shown in Figure 2, creating two levels of control. First, the high level VSC control is simulated at 1 kHz with perfect feedback to tune the sliding mode control strategy. Next, the lower PD control at 10 kHz is added to the simulation. Finally, perfect feedback is replaced by estimated states obtained from a Kalman filter.

Higher Level Control (VSC) Simulation

The first step in simulation is to discretize the system model using a first order hold to approximate the RASID. The discretized matrices are then transformed into regular form using

$$T=\begin{bmatrix}1 & 0 & 0 & \frac{-b_1}{b_4}\\ 0 & 1 & 0 & \frac{-b_2}{b_4}\\ 0 & 0 & 1 & \frac{-b_3}{b_4}\\ 0 & 0 & 0 & 1\end{bmatrix}$$

The sliding surface is then calculated using LQR, with $Q=diag[0 \quad 1 \quad 0]$, which penalizes the tip position, and $r=1$, which penalizes the control effort. To calculate the control gains, (12) is used to obtain an upper bound for α_i and a lower bound for β_i. In order to obtain an exact value, a fixed positive number, ε, is added or subtracted to each of the bounds. Initially, ε is chosen to be 5.

Once the surface and control gains are calculated, they can be used to control the system so that the tip follows a specified trajectory. This trajectory is obtained using the existing computer software that calculates a jerk-limited path from one point to the next. In this case, a repetitive motion between the home position, 0, and 55 mm is used, as shown in Figure 3.

An error vector, $E(k)$, is calculated using the desired position at the kth timestep. Since the tip position error is the only penalized state in the cost function, the error vector is calculated assuming the desired position and velocity of the base mass are the same as that of the tip. Thus, $E(k)=[x_1 \quad x_2 \quad \dot{x}_1 \quad \dot{x}_2]^T-[x_d \quad x_d \quad \dot{x}_d \quad \dot{x}_d]^T$. The error vector is used to first calculate the sliding surface, $\sigma=SE$, and then the gain matrix, K, using e_i instead of x_i. Finally, the input, $u=KE$, is used to obtain the next set of state values where $X(k+1)=AX(k)+Bu$. This process continues for every desired point of the trajectory.

Initial simulations had a maximum tracking error of about 0.4 mm. To improve tracking, the penalty on tip position could be increased by reducing r or increasing the nonzero term of Q. However, since the actual system can only output a maximum force of 100 N, the error can only be reduced to 0.02 mm, as seen

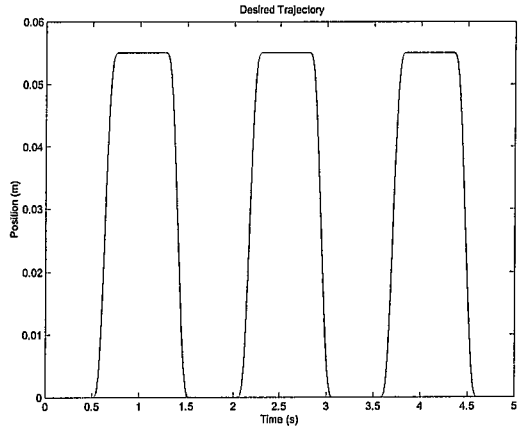

Figure 3. Desired Trajectory used for Simulation

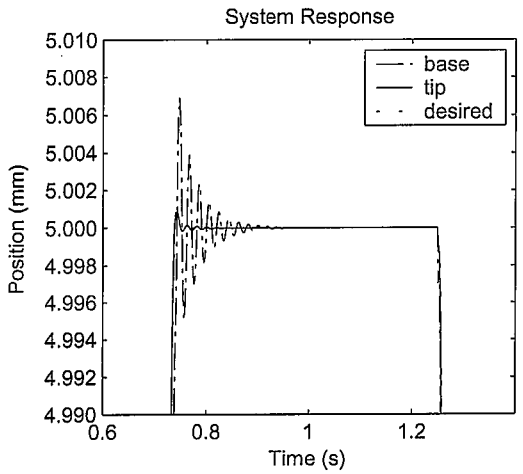

Figure 4. VSC Simulation with Perfect State Feedback

in Figure 4. Altering ε can also affect the time response since the system will respond faster as ε is increased. However, the control effort is increased and there are more induced vibrations that result in increased switching of the control signal. Thus, choosing a smaller value of ε and altering the sliding surface seems to be the best approach to tuning the controller.

Low Level Control (PD) Simulation

To add the RASID's PD control to the simulation, the force input calculated by the VSC controller must be converted into a desired position, r, that serves as an input to the RASID. This is done by equating the force to the proportional and derivative gains, resulting the discrete equation, $u(k) = K_p[r(k) - x_1(k)] + K_d[r(k) - r(k-1) - x_1(k) + x_1(k-1)]$. Upon rearranging, an expression for $r(k)$ can be obtained as follows.

$$r(k) = \frac{u(k) + K_d r(k-1) + (K_p + K_d)x_1(k) - K_d x_1(k-1)}{K_p + K_d} \tag{13}$$

To simulate the 10kHz PD loop, intermediate control values must be determined for simulation purposes. Since the RASID uses linear interpolation, the intermediate points are found by incrementing $u(k-1)$ by $\frac{(u(k)-u(k-1))T_{10kHz}}{T_{1kHz}}$ until $u(k)$ is reached. These values are then used in (13) to calculate the intermediate control values.

The new states can then be calculated using $X(k+1) = \hat{A}X(k) + \hat{B}[K_p \quad K_d][r \quad \dot{r}]^T$, where $\hat{A}$ and $\hat{B}$ are discretized at 10 kHz using a zero-order hold. It is important to note that the sliding surface and control gains are still calculated using discretized matrices at 1 kHz with a first-order hold. Adjusting r so that the control effort remained under 100 N, the tracking error is about 0.023 mm.

Simulation Using Estimated States

The final step is to obtain state estimates using the outputs instead of using perfect feedback. Since the vision measurements are not available at all times and are delayed by a significant number of time steps, a multirate Kalman Filter, developed by Mashner [13], is used. In addition to the system model, the filter requires the specification of other parameters, listed in Table 2.

The vision frequency and delay were estimated based on knowledge of the vision system to be used for experiments. The input covariance is multiplied by a factor relating to the unknown noise in the amplifier. The output covariance matrix is obtained by assuming that the covariance of each sensor is independant, thus it becomes diagonal.

The outputs are calculated using $y(k) = CX(k) + Bu(k)$ with the states obtained from $X(k) = AX(k-1) + Bu(k-1)$. The filter calculates the estimated states using the simulated outputs, which are then used to obtain the control value for the next time step. The results are shown in Figure 5. As expected, the tracking error is not as good since the estimates are used, leading to a maximum error of 0.15 mm.

Although the results in the previous simulations are acceptable, there are considerable oscillations of the base mass during

Vision meas. frequency	30 Hz
Vision meas. delay	25 ms
Input covar. matrix	$(0.01)BB^T(0.01)$
Output covar. matrix	diag[2.08e-12 2.41e-3 2.03e-9]

Table 2. Kalman Filter Parameters

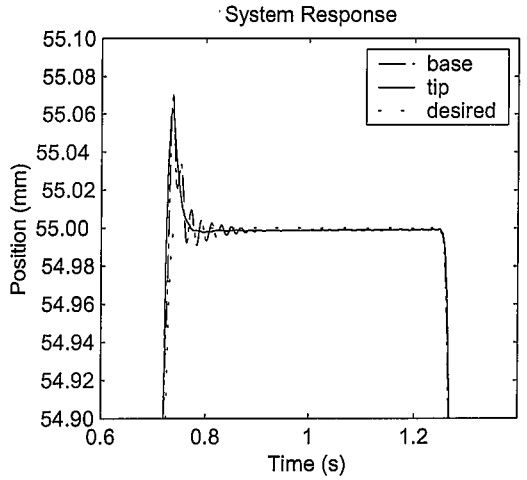

Figure 5. VSC Simulation with Kalman Filter

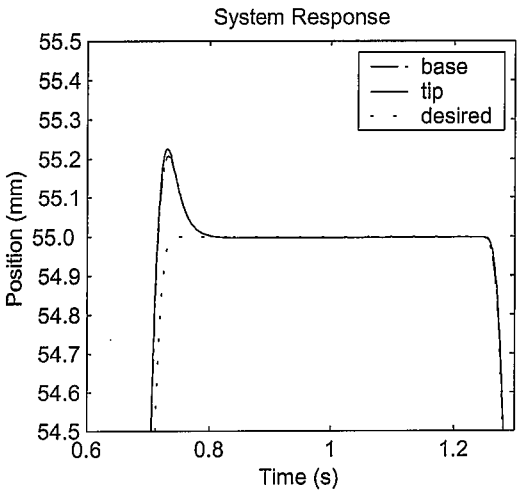

Figure 6. Simulation with x_2 & v_1 Penalized

the control process. Since this may not be desirable on an actual system due to limits on the motor's response time, the penalization of base velocity was investigated. Thus, Q is altered to contain two non-zero diagonal terms. The term corresponding to the velocity is chosen to be the same as r so that the tip position remains the most penalized term. The results, notably the reduction of bass mass vibrations, are shown in Figure 6. The percent overshoot is about 0.36%.

Robustness of Control Strategy

Up to this point, the simulations have been done asuming a perfect model. To examine the robustness of the control method, the $\hat{A}$ and $\hat{B}$ matrices were calculated using altered parameters before being discretized. Since the variation initially caused the input to be above 100 N, the saturation of the motor was added to the simulation. Each parameter was varied from 10% to 200% of the nominal value and the ranges in which the tracking error remained less than 1 mm with perfect state feedback are listed in Table 3. Perfect feedback is used to isolate the control method since the filter also uses an assumed model.

The preceding simulation results verify that the control method can achieve an acceptable level of tracking control. They also indicate that the choice of Q and r in the cost function directly impacts the behavior of the closed loop system and must be chosen carefully. For example, the overshoot and oscillations are reduced when the base velocity was penalized. Finally, the robustness to paramater variations was also verified through simulations.

Experiments

The structure used to test the developed control algorithm consists of a rectangular block of steel attached to the end of a 1.5 m long piece of extruded aluminum. A notch is cut near the mounted end of the aluminum to increase its flexibility. The structure is mounted to an Anorad LW-10 linear stage that contains a brushless linear motor powered by an Anorad High Voltage Brushless Servo Amplifier configured to run in current mode.

The sensors used include an Anorad MER-50 encoder that is embedded into the stage to measure the position of the base plate with a resolution of 1μm. A MEMS-type AXDL50EM-3 Analog Devices accelerometer with a +/- 4 G resolution is attached to the steel block. Finally, a DVT Camera with strobe is used to measure the tip's position by detecting a strip of reflective tape on the steel block.

Since CAMotion would like to incorporate this new control algorithm into their existing software, the algorithm was added to the existing graphical user interface (GUI) software with the aid of CAMotion's engineers. Mashner's filter was also incorporated into the software, making the estimated states available for the control signal calculations. In order to obtain estimated

m_1	40%-140%	r	45%-200%
m_2	25%-105%	L	75%-102%
k	30%-135%	I	96%-175%
b	10%-200%		-

Table 3. Robustness Ranges for Pendulum Model Parameters

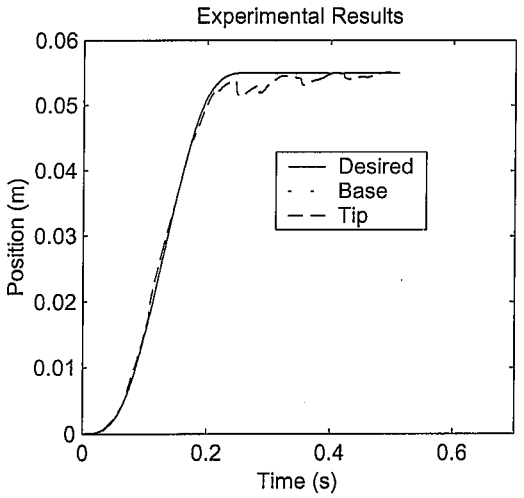

Figure 7. Experimental Results

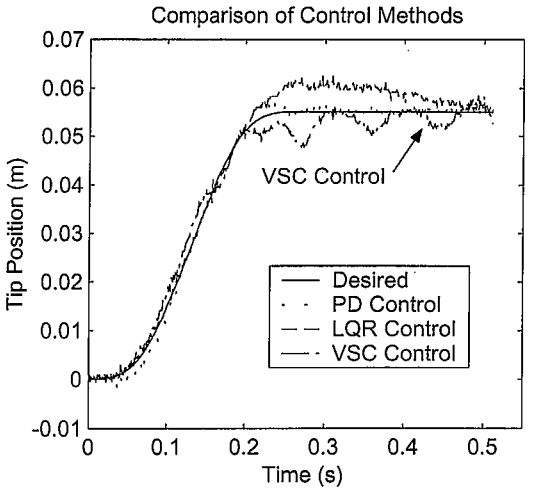

Figure 8. Comparison of Control Methods

values with the correct units, the sensor outputs had to be converted into proper units for the filter calculations. Furthermore, the control effort had to be converted into the correct units before being output to the RASID.

The variable structure control algorithm was then tested using the same 55 milimeter jerk-limited trajectory used in the simulations. Using $r = 0.001$ and $Q = diag[0 \quad 100 \quad 0.001]$, the following sliding surface and control gains are obtained.

$$S = [138.55 \quad -59.665 \quad -0.5562 \quad 2.1303]$$
$$\alpha = [-5,325,907 \quad 3,414,075 \quad 8,517.5 \quad -48,587]$$
$$\beta = [-5,325,897 \quad 3,414,085 \quad 8,527.5 \quad -48,577]$$

Figure 7 shows the results of this testing, which are not as good as indicated by simulation. This may be a result of modeling uncertainties, which affect the performance of the Kalman filter and control algorithms. Also, there are time delays of about 2 ms on the encoder and accelerometer measurements due to the use of the RASID, which transmits the collected data via a USB cable, that are not accounted for in the control algorithm that may result in time responses that differ from the simulations.

To verify that the test system was set-up correctly, it was run using the existing PD control of the RASID in conjunction with CAMotion's GUI trajectory planning software. A laser measurement device was used to record the tip position using an oscilloscope. Next, data was collected using an LQR control approach from work done by Mashner on the same system [13]. Laser measurement data was also taken with the variable structure control and compared with the other control methods, as shown in Figure 8.

Neither state feedback methods track the desired tip position better than the current RASID PD controller, as verified by mean squared error calculations. However, the variable structure control method has a smaller mean squared error than the LQR method. Thus, the method developed in this thesis performs better than the LQR feedback method when using the same state estimator. The poor performance of the state feedback methods when compared to the PD controller may be a result of poor estimates from the Kalman filter or significant time delays in the sensor measurements since the PD control is done in the RASID, not on the computer. Also, the Kalman filter design is based on the selection of noise covariances that are approximated based on anticipated model uncertainty and measurement discretization. Thus, it is uncertain that the most suitable values were selected for these experiments and further investigation is needed to improve the system's performance.

The final experiment that was conducted was to verify the robustness of this control strategy. Since there were numerous slender rectangular pieces of aluminum readily available, these were added to the bottom of the steel block to increase the tip mass. Two trials were run, one with a 10.5% increase in mass and the other with a 15.8% increase, using the same gains stated earlier. The resulting responses remained stable and the mean squared error was on the same order of magnitude as before.

Conclusions

A new tracking control method has been developed and proven to achieve acceptable tracking results. Although it did not perform better than PD control, it did achieve better tracking results than LQR control for the same system with the same

filter.

The control algorithm has been proven to be less sensitive to changes in the actual system, resulting in increased robustness with acceptable tracking results. Robustness is one of the major contributions of this work because flexible system models usually contain uncertainties due to truncation of flexible modes, small angle approximations, etc. Furthermore, the method has also been generalized so that it can be applied to any controllable, linear, state-space system. Finally, the model used, although not new, has not been widely investigated in VSC research. The use of this model may be favorable because it results in a more intuitive model that is easier to explain to non-specialists and is adequate for the experimental system of interest, where most compliance is concentrated at a weak spot along the beam.

Although the control method presented has been proven to be an acceptable tracking control strategy, there are some ways in which the results could be improved. For example, perfect tracking is not achievable since the desired trajectory is designed for a rigid system, i.e. the base motion. Thus, if a better trajectory is planned that is achievable for the tip mass, tracking results could be greatly improved. Also, the use of LQR to select the sliding surface gains could be replaced by another feedback control method, such as pole placement. Since the sliding surface is critical in the system's time response, a different design method my lead to more favorable responses. Finally, the application of adaptive learning control or input shaping in conjunction with variable structure control is another issue that could be explored.

REFERENCES

[1] W.T. Quian and C.C.H. Ma. Weighted sliding mode control of a flexible one-link arm. In *IEEE Pacific Rim Conference on Communications*, Computers and Signal Processing, pages 162–165, May 1991.

[2] W.T. Quian and C.C.H. Ma. A new controller design for a flexible one-link manipulator. *IEEE Transactions on Automatic Control*, 37(1):132–137, January 1992.

[3] Susy Thomas and B. Bandyopadhyay. Comments on "a new controller design for a flexible one-link manipulator". *IEEE Transactions on Automatic Control*, 42(3):425–429, March 1997.

[4] Jeang-Lin Chang and Yon-Ping Chen. Force control of a single-link flexible arm using sliding-mode theory. *Journal of Vibration and Control*, 4:187–200, 1998.

[5] Xinkai Chen and Guisheng Zhai. Sliding mode method based vibration control of flexible arms. In *American Control Conference*, pages 2374–2379, May 2002.

[6] Dadi Hisseine and Boris Lohmann. Nonlinear tracking control for a lightweight flexible robot. In *IEEE International Conference on Systems, Man, and Cybernetics*, volume 5, pages 3360–3365, October 2000.

[7] Harry N. Iordanou and Brian W. Surgenor. Experimental evaluation of the robustness of discrete sliding mode control versus linear quadratic control. *IEEE Transactions on Control Systems Technology*, 5(2):254–260, March 1997.

[8] Nader Sadegh, Ai-Ping Hu, and Courtney James. Synthesis, stability analysis, and experimental implementation of a multirate repetitive learning controller. *ASME Journal of Dynamic Systems, Measurement, and Control*, December 2002.

[9] R.A. DeCarlo, S.H. Zak, and S.V. Drakunov. *The Control Handbook*, chapter 57.5 Variable Structure, Sliding-Mode Controller Design, pages 941–951. CRC Press, 1996.

[10] Jean-Jacques E. Slotine and Weiping Li. *Applied Nonlinear Control*. Prentice Hall, 1991.

[11] Raymond A. DeCarlo, Stanislaw H. Zak, and Gregory P. Matthews. Variable structure control of nonlinear multivariable systems: A tutorial. In *Proceedings of the IEEE*, volume 76, pages 212–232, March 1988.

[12] K. David Young and Umit Ozguner. A control engineer's guide to sliding mode control. *IEEE Transactions on Control Systems Technology*, 7(3):328–342, May 1999.

[13] Michael Mashner. Multirate machine vision based kalman filtering and state feedback control. Master's thesis, Georgia Institute of Technology, November 2002.